The evolution of a Müllerian mimic in a spatially distributed community

Mathieu Joron[a,b,*], Yoh Iwasa[c]

[a]Institut des Sciences de l'Evolution, Université de Montpellier, Place Eugène Bataillon, 34095 Montpellier Cedex 05, France
[b]Department of Biology, University College London, 4 Stephenson Way, NW1 2HE, London, UK
[c]Department of Biology, Faculty of Sciences, Kyushu University, Fukuoka 812-8581, Japan

Abstract

Strong positive density-dependence should lead to a loss of diversity, but warning-colour and Müllerian mimicry systems show extraordinary levels of diversity. Here, we propose an analytical model to explore the dynamics of two forms of a Müllerian mimic in a heterogeneous environment with two alternative model species. Two connected populations of a dimorphic, chemically defended mimic are allowed to evolve and disperse. The proportions of the respective model species vary spatially. We use a nonlinear approximation of Müller's number-dependent equations to model a situation where the mortality for either form of the mimic decreases hyberbolically when its local density increases. A first non-spatial analysis confirms that the positive density-dependence makes coexistence of mimetic forms unstable in a single isolated patch, but shows that mimicry of the rarer model can be stable once established. The two-patch analysis shows that when models have different abundance in different places, local mimetic diversity in the mimic is maintained only if spatial heterogeneity is strong, or, more interestingly, if the mimic is not too strongly distasteful. Therefore, mildly toxic species can become polymorphic in a wider range of ecological settings. Spatial dynamics thus reveal a region of Müllerian polymorphism separating classical Batesian polymorphism and Müllerian monomorphism along the mimic's palatability spectrum. Such polymorphism-palatability relationship in a spatial environment provides a parsimonious hypothesis accounting for the observed Müllerian polymorphism that does not require quasi-Batesian dynamics. While the stability of coexistence depends on all factors, only the migration rate and strength of selection appear to affect the level of diversity at the polymorphic equilibrium. Local adaptation is predicted in most polymorphic cases. These results are in very good accordance with recent empirical findings on the polymorphic butterflies *Heliconius numata* and *H. cydno*.
© 2005 Elsevier Ltd. All rights reserved.

Keywords: Müllerian mimicry; Toxicity; Spatial heterogeneity; Density-dependence; Local adaptation

1. Introduction

Traits under positive frequency- or density-dependence should not evolve polymorphisms. Indeed, the fitness of a self-reinforcing phenotype is by definition minimal when rare and maximal when common, which should lead to the exclusion of all but one phenotype in any locality. Ecologists and evolutionists have focused their attention on negatively frequency-dependent mechanisms, that may lead to protected polymorphisms at the intraspecific level (Ayala and Campbell, 1974; Haldane and Jayakar, 1963; Gigord et al., 2001 for a case study) and to stable coexistence at the community level (e.g. Bever, 1999; Tilman, 1990, review in Chesson, 2000). However, many ecological situations can cause direct self-reinforcement in some traits, such

*Corresponding author. Present address: Institute of Evolutionary Biology, University of Edinburgh, Ashworth Laboratories, King's Buildings, West Mains road, Edinburgh EH9 3JT, UK.
Tel.: +44 131 650 7403; Fax: +44 131 650 6564.
E-mail addresses: mathieu.joron@ed.ac.uk (M. Joron), yiwasscb@mbox.nc.kyushu-u.ac.jp (Y. Iwasa).

as mutualistic host specificity in mycorrhizal fungi (Bever, 1999) or cooperative breeding in birds (Courch-amps et al., 1999). Even simple assortative mating, like pollinator-mediated homogamy in flower colour, may lead to positive density-dependence (Smithson and Macnair, 1997).

Warning coloration leads to density-and frequency-dependent selection (Turner, 1984), like many processes involving signal recognition (Endler, 1988; Nowak and Krakauer, 1999). Warningly coloured prey advertize their distastefulness via conspicuous (or aposematic) colours that are learnt by the predators and subse-quently avoided. Consequently, rare phenotypes are not recognized as unpalatable by predators and are there-fore selected against. In this sense, aposematic coloura-tion is perhaps one of the clearest examples of a self-reinforcing trait, which leads to phenotypic convergence across species boundaries in unpalatable prey (Müller-ian mimicry, Müller, 1879) and to parasitic mimicry by palatable prey (Batesian mimicry, Bates, 1862). Müller-ian mimicry, the adaptive resemblance of defended prey, therefore provides the interspecific evidence for selection towards the locally common signals in warningly coloured prey.

Under positive density-dependence, the evolution of diversity in warning colour and Müllerian mimicry is not predicted by theory: all unpalatable species of a similar size in a locality are predicted ultimately to converge on a single, locally best-protected color-pattern (Mallet and Joron, 1999). However, although most warningly coloured prey are indeed monomorphic locally, diversity is found at all taxonomic levels and geographical scales. Species radiate in different colour races over their distribution ranges, coexisting species belong to diverse mimetic groups within a locality, and some distasteful species even have multiple mimetic forms within a population (see Joron and Mallet, 1998 and references therein). In contrast, polymorphism is expected in Batesian mimicry, where edible prey mimic defended prey. Since they are parasitic to the warning function of the signal, Batesian mimics are under negative frequency-dependence and polymorphism is indeed often observed (e.g. Gordon and Smith, 1998; West, 1994).

Since experimentation on the benefits of mimicry in nature have proved difficult (but see Benson, 1972; Kapan, 2001), the dynamics of mimicry have often been studied via mathematical or simulation models. Authors have usually concentrated on identifying the possible mechanisms in prey evolution or predators' psychology that could lead to warning colour diversification in the face of a theoretically strong homogenizing selection (Gavrilets and Hastings, 1998; Huheey, 1988; Owen and Owen, 1984; Speed, 1993; Turner et al., 1984; see Joron and Mallet, 1998 and references therein). However, the conclusions of these studies are highly dependent on the assumptions regarding the behaviour of predators, particularly their learning and forgetting functions (Speed and Turner, 1999; Turner and Speed, 1996).

More importantly, all authors looked for mechanisms that could maintain prey diversity within a population, and left aside the potential role of space. The idea that environmental heterogeneity could maintain mimetic diversity was verbally proposed by Brown and Benson (1974), and has received recent empirical support (Joron et al., 1999; Kapan, 2001). Spatial variation in the abundance of species or forms with different warning patterns should indeed translate into even greater fitness variations for the different mimics.

Here, we carry out one of the first theoretical studies of Müllerian mimicry that takes into account spatial heterogeneity, to explore the conditions under which diversity may emerge and be maintained in a mimic (see also Sasaki et al., 2002 on mimicry and moving clines). We propose an analytical model for a two-patch system where the dynamics of two conspecific mimetic forms are analysed in response to four factors: unpalatability (which affects the strength of positive density-depen-dence), the migration rate between patches, the overall abundance of model species (which affects the average protection that the mimic enjoys due to mimicry) and the level of spatial heterogeneity in the relative abundance of the models of the two colour-patterns. We compare the dynamics of the one-and two-patch systems to highlight that taking space into account can be of crucial importance in explaining why some distasteful species are polymorphic and how the different mimicry rings may coexist. Our results match especially well recent empirical data on the spatial pattern of selection in one of the most polymorphic Müllerian mimics known, the butterfly *Heliconius numata* (Joron et al., 1999).

2. Model and assumptions

We consider two adjacent habitat patches containing several defended species. One of these (haploid) species, hereafter called the 'mimic', can be of two forms, A and B, which are identical except for colour pattern. N_{ij} is the density of mimics of form i ($i =$ A, B) in patch j ($j =$ 1, 2). Two or more other distasteful species, called 'models', occur in each patch, each of which has one colour pattern A or B, copied by the mimic. In the present study, the models constitute a fixed part of the mimic's "mimetic environment" and their density is not allowed to evolve. Their local abundance is therefore not referred to by specific variables, but affects the mortality of A and B mimics in each patch (see below). Our model is an ecological model, or, if viewed as genetic, a haploid model without complications due to dominance, epistasis and other genetic interactions. For

a genetically explicit model of mimicry, see Mallet and Barton, 1989.

We follow the dynamics of the two forms of the mimic only. The total change in density of form i in patch j, dN_{ij}/dt, is the sum of the change due to mortality, D_{ij}, the change due to migration between the two patches, M_{ij}, and the change due to reproduction and competition, G_{ij}. These three factors are detailed below.

2.1. Mortality

2.1.1. Density-independent mortality, patch-dependent mimetic protection

The environment is heterogeneous for mimicry, i.e. the mimetic protection for each colour form is spatially variable. This is the case when the model species are not evenly distributed among habitat patches, e.g. if type-A models are more abundant than type-B models in patch 1, and vice versa in patch 2. These differences could stem, for instance, from narrow ecological requirements of the different model species, competitive exclusion, or some kind of Allee effect. Such spatial heterogeneity is found for instance in the regional distribution of ithomiine species in the Amazon basin, especially *Melinaea* and their associated tiger-patterned mimicry rings, including polymorphic species like *H. numata* (Beccaloni, 1997; Brown and Benson, 1974; Joron et al., 1999). Initially, we assume equal total density of models in both habitats, but we investigate asymmetrical cases later on.

Being distasteful to predators, the models generate protection for the mimic regardless of the mimic's palatability. In this analytical study, the models' abundance is not allowed to change with time, so their protective effect on the mimic is a constant that we can include in the "basic mortality factors" d_{ij} of the two mimetic forms (for form i in patch j). For instance, if A models are more abundant than B models in patch 1, then A mimics suffer a lower basic mortality than B mimics in this patch: $d_{A1} < d_{B1}$. Conversely, in patch 2, $d_{A2} > d_{B2}$.

2.1.2. Density-dependent mortality

Most population genetics and simulation models on mimicry used a linear approximation for the frequency-dependent function: the fitness of each form was assumed to be proportional to its frequency in the population (see Gavrilets and Hastings, 1998; Mallet, 1986b; Mallet and Barton, 1989; Sasaki et al., 2002; Speed, 1993). However, because the proportion of mimics eaten during predator learning should not increase linearly with mimic density, Mallet and Joron (1999) recently suggested a more realistic density-dependent function derived from the first mathematical model of mimicry by Müller (1879). This model is called

"number-dependent" because predators need to sample a certain number ("n_k") of a prey form per unit time to learn and avoid it. This idea has recently received some experimental support (Lindström et al., 2001): although probably not fixed in nature, n_k does not increase linearly with population density; the predation rate becomes a strongly nonlinear, hyperbolically decreasing function of relative prey density in the population (Lindström et al., 2001; Mallet and Joron, 1999). Under such nonlinear density-dependence, selection against very rare forms should be enhanced at very low frequencies, but should in be weakened at intermediate frequencies, thus potentially greatly affecting the maintenance of mimetic polymorphism (Mallet and Joron, 1999).

To account for such nonlinear density-dependence, the basic mortality factors d_{ij} is multiplied by $1/(1 + lN_{ij})$ which produces a hyperbolic decrease in mortality with the density of form i when $1 > 0$. The mortality, or change in density of form i in patch j due to local predation, is

$$D_{ij} = -\frac{d_{ij}}{1 + lN_{ij}} N_{ij} \tag{1}$$

Thus, Müller's n_k (1879)—the total number of prey killed per unit time due to predator inexperience—is equivalent to d_{ij}/l when N_{ij} is large. Here, l represents the mimic's unpalatability: for positive values of l, mimics are unpalatable and favour their own survival (positive feedback through predators' learning); if l is negative, mimics are palatable and have a deleterious effect on their own survival. Here we restrict our analysis to the case $l > 0$, for which the local maintenance of diversity is not predicted by theory. Mortality is highest when few individuals are present (maximum at d_{ij}), declines nonlinearly, and asymptotically approaches 0 when the density is high.

Nonlinear positive density-dependence affects the invasibility of the monomorphic equilibrium and the stability polymorphic equilibria in the two-patch system, in a way that is largely absent from classical theory on the coexistence in spatially heterogeneous populations with limited migration (Hedrick, 1986; Karlin and McGregor, 1972; Levin, 1976), where emphasis was given to directional selection within habitats or patches or competitive interactions entailing mostly negative density-dependent effects.

2.2. Migration and local demography

Mimics migrate between patches at a rate m. The change in density of form i due to migration is therefore $M_{i1} = m(N_{i2} - N_{i1})$ in patch 1 and $M_{i2} = m(N_{i1} - N_{i2})$ in patch 2. The two forms within the mimetic species are assumed to compete with each other locally in either

patch. The change in density of mimic i in patch j due to local competition is chosen as a logistic regulation rule

$$G_{ij} = rN_{ij}[1 - (N_{Aj} + N_{Bj})/K], \tag{2}$$

where r is the intrinsic growth rate and K the carrying capacity in the patch. These factors are assumed equal across patches.

2.3. Realism and coevolution

In order to include realistic assumptions concerning the spatial dynamics and the nonlinearity of the density-dependence, while keeping the model analytically tractable, we chose to make the model simple with respect to coevolutionary dynamics. Spatially explicit model-mimic coevolutionary simulations would be an important counterpart to our results for the cases where coevolution is likely. However, we explain below why our model should be realistic in most cases.

It may seem unrealistic to consider a fixed abundance of models in the equations, because it is intuitive to think of Müllerian mimicry as a mutualistic, reciprocal interaction. However, there are theoretical and empirical reasons why Müllerian mimicry is and should be one-sided in the real world (for a review, see Mallet, 1999). Theoretical studies show that the benefits of Müllerian mimicry are much higher for the rarer species (Müller, 1879), or the less distasteful species (Mallet, 1999), so the distinction between model and mimics is not arbitrary; stronger selection in the mimic translates into a unilateral evolution of the mimicry (Turner, 1977, 1984; Mallet, 1999). Empirically, all mimic species studied have been interpreted to have evolved unidirectionally, and phylogenetic, phylogeographic, and experimental evidence from diverse Müllerian mimicry communities (two- or many-species systems) all point to a lack of coevolution (see e.g. Brower, 1996; Flanagan et al., 2004; Mallet, 1999; Plowright and Owen, 1980; Symula et al., 2001). For these reasons, we chose to concentrate on mimic evolution rather than theoretical model-mimic coevolution in this study. This in our view remains largely realistic, insofar as it amounts to assuming that the models are numerous compared to the focal species or more strongly unpalatable (Mallet, 1999; Müller, 1879), which is commonly the case in nature (see e.g. Brown and Benson, 1974; Chai, 1986; Kapan, 2001; Mallet, 1993; 1999). This assumption allowed us to put the emphasis on improving the realism of other aspects which have more empirical support than coevolution, specifically spatial dynamics and nonlinear density-dependence. For a coevolutionary model of mimicry in a single population and assuming linear frequency-dependence, see Gavrilets and Hastings (1998).

2.4. Final dynamical system

The total change in density of form i in patch j is $dN_{ij}/dt = D_{ij} + G_{ij} + M_{ij}$. We rescaled all variables to growth rate and carrying capacity, as follows: $x_j = N_{Aj}/K$, rescaled density of form A in patch j; $y_j = N_{Bj}/K$, rescaled density of form B in patch j. $\lambda = lK$, rescaled density-dependence factor; $\delta_{ij} = d_{ij}/r$, rescaled mortality for form i in patch j; $\mu = m/r$, rescaled migration rate; and $\tau = tr$, rescaled time unit. The rescaled variables are dimensionless. The dynamical system becomes

$$dx_1/d\tau = -\frac{\delta_{A,1}}{1+\lambda x_1}x_1 + (1 - x_1 - y_1)x_1 + \mu(x_2 - x_1),$$
$$dy_1/d\tau = -\frac{\delta_{B,1}}{1+\lambda y_1}y_1 + (1 - x_1 - y_1)y_1 + \mu(y_2 - y_1),$$
$$dx_2/d\tau = -\frac{\delta_{A,2}}{1+\lambda x_2}x_2 + (1 - x_2 - y_2)x_2 + \mu(x_1 - x_2),$$
$$dy_2/d\tau = -\frac{\delta_{B,2}}{1+\lambda y_2}y_2 + (1 - x_2 - y_2)y_2 + \mu(y_1 - y_2).$$
$$\tag{3}$$

2.5. Preliminary results: Single patch dynamics

In a single isolated patch, the system is considerably simplified

$$dx_0/d\tau = -\frac{\delta_A}{1+\lambda x_0}x_0 + (1 - x_0 - y_0)x_0,$$
$$dy_0/d\tau = -\frac{\delta_B}{1+\lambda y_0}y_0 + (1 - x_0 - y_0)y_0, \tag{4}$$

where the subscript 0 refers to the behaviour in a single population. By standard local linearization procedure, we prove that no coexistence is stable when the mimic is unpalatable: only one form can reside. Is such single-form equilibrium robust to replacement by the other colour type? Two situations may occur: (i) the resident has the pattern of the locally most abundant model (i.e. is ultimately better suited to the local mimetic environment); in this case, it is easy to show that a less favoured form cannot invade. (ii) The resident has the pattern of the locally less abundant model; in this case, the rare variant is ultimately better suited than the resident to the mimetic environment, but the resident enjoys some immediate density-dependent advantage. The variant may however invade depending on some condition on λ, δ_A and δ_B: we show (Appendix A) that there exists a threshold value λ_0 above which A cannot invade, defined as

$$\lambda_0 = \frac{\delta_B - \delta_A}{\delta_A(1 - \delta_A)}. \tag{5}$$

If $\lambda < \lambda_0$, e.g. for mild unpalatability (note that the forms A and B have the same unpalatability λ), A invades and replaces B; in that case there is a single stable equilibrium, where only the form that mimics the commoner model can resist replacement. In contrast, if $\lambda > \lambda_0$, there is a bistable equilibrium where one form or the other may dominate the patch and is robust to

invasion by a rare alternative form. In that case, e.g. for strong unpalatability, the focal species may mimic either the rarer or the commoner model species, depending on initial conditions (numerical results not shown, but see the two-patch analysis below).

2.6. Spatial analysis: Two symmetrical populations

In the two-patch analysis that follows, we focus on the simple symmetrical case in which $\delta_{A1} = \delta_{B2}$ (low mortality, good mimetic protection) and $\delta_{A2} = \delta_{B1}$ (high mortality, low protection). This means that the total number of A *models* in patch 1 equals the total number of B *models* in patch 2. Thus, the mean basic mortality for the mimic, δ, is equal in both patches. It is convenient to rewrite the δ_{ij} parameters as follows: $\delta_{A1} = \delta_{B2} = \delta(1 - \sigma)$ and $\delta_{A2} = \delta_{B1} = \delta(1 + \sigma)$. The parameter σ is therefore a "habitat heterogeneity" parameter, i.e. a measure of the relative environmental difference between the two patches. Eq. (5) becomes

$$\lambda_0 = \frac{2\delta\sigma}{\delta(1 - \sigma)[1 - \delta(1 - \sigma)]}. \tag{6}$$

In the analysis, we will first derive analytical expressions of the stability conditions around equilibria. We will then search numerically for the location of the stability/instability boundaries for all parameter combinations.

3. Monomorphic equilibria in a two-patch system

3.1. Invasibility condition

If mimics of form A only are present at equilibrium $\{(\hat{x}_1, 0), (\hat{x}_2, 0)\}$, mimics of form B can increase and establish in the two-patch system if and only if (see Appendix B.1)

$$(-\delta_{B1} + 1 - \hat{x}_1 - \mu)(-\delta_{A1} + 1 - \hat{x}_2 - \mu) < \mu^2 \tag{7}$$

Note that the equilibrium values $\hat{x}_1$ and $\hat{x}_2$ depend on the unpalatability parameter λ. As in the one-patch system, there is a critical value λ_c such that form B can establish in its favourable patch when $\lambda < \lambda_c$. We give details on the relationship between this invasibility boundary λ_c and the migration rate μ in the following paragraph.

3.2. Shape of the invasibility boundary

(a) *No migration*, $\mu = 0$: At null migration (closed patches), Eq. (7) becomes

$$(-\delta_{B1} + 1 - \hat{x}_1)(-\delta_{A1} + 1 - \hat{x}_2) < 0 \tag{8}$$

From the results for a single patch, we know that the alternative form may invade only in its favourable

patch, as long as the condition $\lambda < \lambda_0$ is met (Eq. (5)). This value λ_0 is strictly positive, showing there always exists a positive λ (smaller than λ_0) for which monomorphic equilibria are not stable.

(b) *Fast migration*: For fast migration, the two-patch system tends to behave like a single large patch with averaged parameters, i.e. with mortality $\delta_\infty = (\delta_{A1} + \delta_{B1})/2 = \delta$. Therefore, the threshold value λ_0 (Eq. (5)) tends towards 0 (formal proof in Appendix B.2). Thus, for fast migration, the monomorphic equilibrium is stable in any unpalatable mimic.

(c) *Migration of intermediate level*: To obtain the values for the monomorphic equilibrium, we searched for the one in which $\hat{x}_1$ and $\hat{x}_2$ are positive and both y_1 and y_2 are zero, using the Newton method for finding roots. This equilibrium was then tested for stability using Eq. (7). This method was repeated spanning the range of possible parameter combinations, to derive the shape of the invasibility boundary as a function of the different parameters. In practice, the critical value of λ beyond which invasion is impossible (denoted here as λ_c) was looked for as a function of migration μ and habitat heterogeneity σ. In particular, λ_c varies from λ_0 for null migration ($\mu = 0$) down to 0 for very fast migration ($y \to \infty$) (Fig. 1a).

As shown above, there is a negative relationship between λ_c and μ. In biological words, this means that in a strongly unpalatable mimic, a second form cannot establish in a two-patch system unless migration is very slow. Conversely, under substantial migration, a second form can establish only if the species is mildly unpalatable (remember both forms have equal unpalatability). In contrast, λ_c increases with habitat heterogeneity σ (Fig. 1b): in a very unpalatable mimic, heterogeneity needs to be more pronounced for a second form to establish.

4. Coexistence of several mimetic forms

4.1. The internal equilibria

Apart from the two trivial monomorphic equilibria studied above, at least one coexistence equilibrium may exist. In particular, because of the symmetry in the equations, the equilibrium where $\hat{x}_1 = \hat{y}_2 (= \hat{x})$ and $\hat{x}_2 = \hat{y}_1 (= \hat{y})$ is expected and can be called symmetric equilibrium. These can be identified numerically. Although we cannot prove analytically that all internal equilibria are symmetrical or that there are no limit cycles, our numerical search failed to find any asymmetrical equilibrium or cycling. Therefore, we study equilibria that have the form $\{(\hat{x}, \hat{y}), (\hat{y}, \hat{x})\}$.
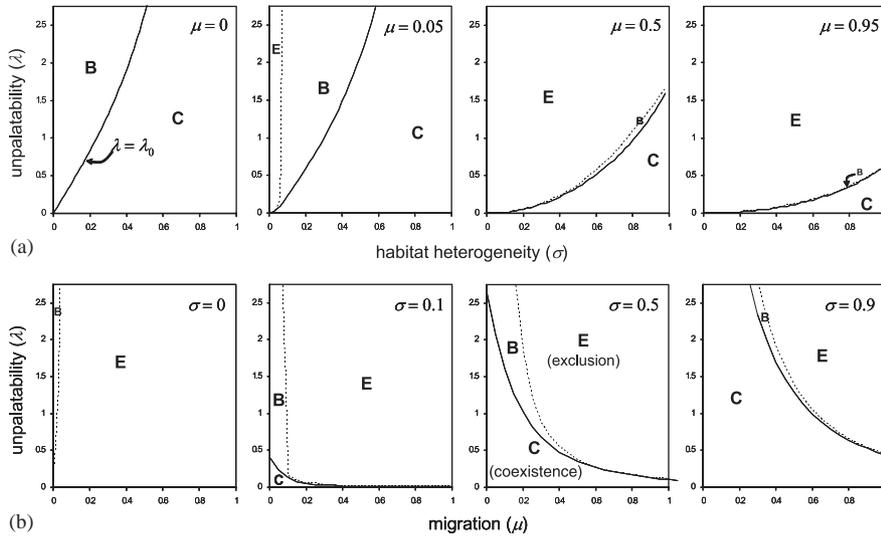
Fig. 1. Exclusion vs. coexistence of mimetic forms in a two-patch landscape. The boundary value of the unpalatability factor λ separating the domains of stable vs. unstable exclusion of one mimetic form (solid line), and the domains of stable vs. unstable coexistence of the two mimetic forms (dotted line), is plotted (a) against the level of habitat heterogeneity σ, for different values of μ and (b) against the level of migration μ for different values of σ. On each graph the two curves divide the space in three zones: stable exclusion of one form (E) (form B cannot increase in numbers from an initially low density), stable coexistence of the two forms (C), and a zone in between where both coexistence and exclusion are stable (B). In the latter case, initial conditions, e.g. perturbation, determine the nature of the equilibrium reached. Note that when migration is fast or habitat heterogeneity sharp, initial conditions hardly affect the nature of the equilibrium. In zone C, in the absence of fluctuations, the polymorphism can be called "protected", since the extinction of one form in either patch is not stable with migration. For all graphs, $\delta = 0.5$.

If there is no habitat heterogeneity ($\sigma = 0$), and if migration is slow enough, two stable coexistence equilibria may exist: (i) patch 1 dominated by form A and patch 2 dominated by form B, or (ii) patch 1 dominated by B and patch 2 dominated by A. If heterogeneity increases (σ small), case (ii) becomes locally maladapted, in the sense that the mimics adopt the colour of the rarer model in each patch, but can be stable as long as local density-dependence offsets the basic habitat difference and migration. In particular, if $\mu = 0$, the patches are independent, and case (ii) can be stable if $\lambda > \lambda_0$ (see single patch analysis). We show in Appendix C.1 that one condition for these two stable equilibria to exist is $\delta \geqslant 8\mu$ (with $\delta < 1$). The parameter space where these equilibria exist is restricted, and vanishes as soon as μ or σ increase, i.e. as soon as the marginal and internal equilibrium boundaries get close (Fig. 1).

The local condition for coexistence is derived from the definition of the symmetrical equilibrium $\{(\hat{x}, \hat{y}), (\hat{y}, \hat{x})\}$ in Eq. (3) (details in Appendix C.2)

$$\left[\frac{-\delta(1-\sigma)}{(1+\lambda\hat{x})^2} + 1 - 2\hat{x} - \hat{y} - \mu \right] \left[\frac{-\delta(1+\sigma)}{(1+\lambda\hat{y})^2} + 1 - 2\hat{y} - \hat{x} - \mu \right]$$
$$- (\mu + \hat{x})(\mu + \hat{y}) > 0 \qquad (9)$$

4.2. Shape of the stability boundary

(a) *No or very slow migration*: If $\mu = 0$, each population behaves as the one-patch model studied above, i.e.

only one form can establish in each patch. A coexistence equilibrium is reached at the global level if in either patch the favoured form dominates; in this case one equilibrium is $\left\{ (\hat{x}_0^{(A)}, 0), (0, \hat{x}_0^{(A)}) \right\}$, where $\hat{x}_0^{(A)}$ is defined by Eq. (4) with $y_0 = 0$. As seen before, this equilibrium cannot be invaded by an initially rare mutant. At null migration however, the other coexistence equilibrium $\left\{ (0, \hat{y}_0^{(B)}), (\hat{y}_0^{(B)}, 0) \right\}$ exists, with $\hat{y}_0^{(B)}$ defined by Eq. (4) with $x_0 = 0$. We saw in the single-patch analysis that this equilibrium can be invaded in both patches by the alternative form if $\lambda < \lambda_0$. In that case, due to the symmetry, the coexistence equilibrium switches to the other (locally adapted) one. Otherwise, the non-optimal equilibrium is stable.

(b) *Very fast migration*: As already stated, the behaviour of a two-patch system with very fast migration tends towards that of a single patch with averaged parameters. We saw earlier that coexistence was unstable in a single patch system as soon as the unpalatability factor λ is positive. We conclude (see Appendix C.3) that no coexistence equilibrium is stable in a two patch system with very fast migration.

(c) *Migration of intermediate level*: We used the Newton method for finding roots to determine the equilibria, to plot the values of λ beyond which coexistence becomes unstable. The same qualitative relationship was found as for the invasibility boundary, with some modulations (Fig. 1). Again, strong

unpalatability and weak habitat structuring tend to destabilize coexistence, but the interaction becomes quantitatively different for slow migration: the coexistence area becomes disproportionately large, making coexistence seemingly very likely. However, we will see in the following section that the domains of attraction of these internal equilibria may get narrow under some conditions, turning mathematically stable equilibria into biologically unstable coexistence.

4.3. Local diversity at equilibrium

To investigate whether the stable polymorphic equilibria found under different parameter conditions would be relevant and detectable in sampled populations, we calculated the equilibria $\{(\hat{x},\hat{y}),(\hat{y},\hat{x})\}$ numerically. Fig. 2 shows the quantity $\hat{x}/(\hat{x}+\hat{y})$, the proportion of the dominating form in a patch (e.g. form A in patch 1), revealing which parameters have a significant quantitative influence on the equilibrium.

Migration (μ) has a large influence on the diversity at equilibrium: fast migration reduces the spatial segrega-

tion, i.e. results in higher local diversity nearly proportional to the level of population mixing (but challenges the stability of coexistence). Mean mortality (δ) also has an important quantitative effect on the coexistence: low mortality allows for high local diversity, but, again, challenges stability. More interestingly, unpalatability (λ) and habitat heterogeneity (σ) have little quantitative effect on the local diversity at equilibrium.

In general, this numerical study shows that robust global coexistence is usually associated with low local diversity, whereas locally diverse equilibria are close to the stability boundary of at least one parameter, making coexistence sensitive to variations of this (these) parameter(s).

4.4. Domains of attraction

Because the internal and marginal stability boundaries do not coincide (λ_c is always higher for the internal than for the marginal equilibria), there is a region of the parameter space where one coexistence equilibrium and two monomorphic equilibria are stable simultaneously,
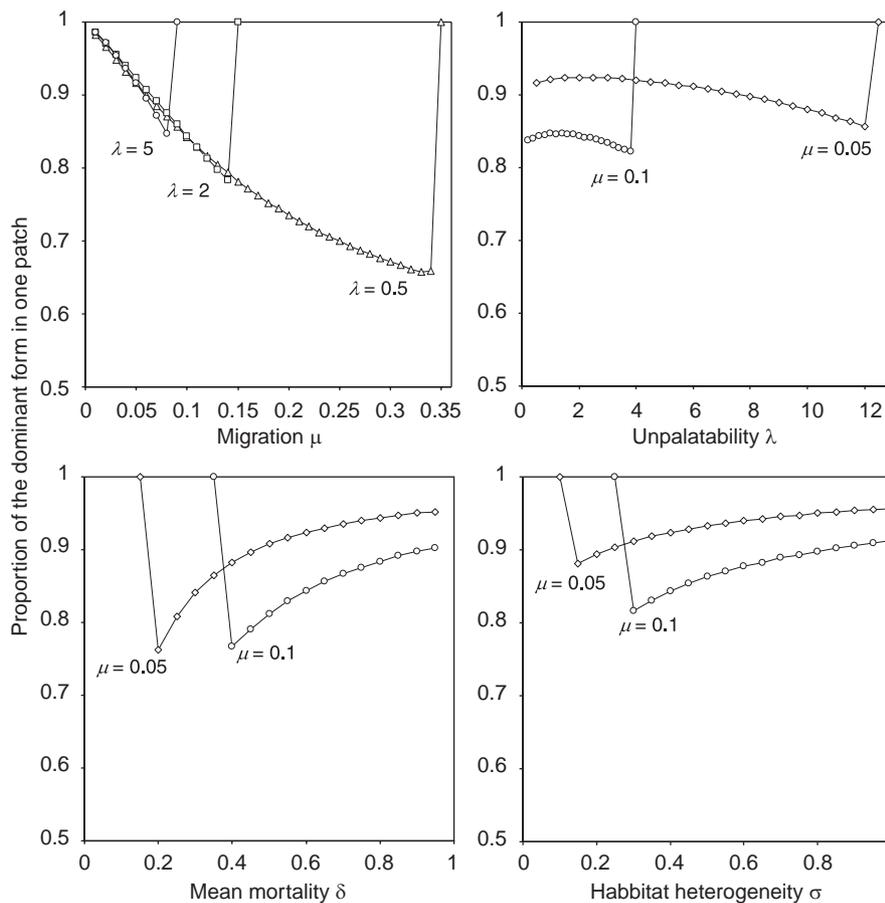

Fig. 2. Local diversity. The proportion of the dominant form in one patch at equilibrium is represented as a function of the different factors of the model. A curve close to 0.5 indicates balanced proportions (high local diversity). Unpalatability (λ) has a very limited effect on the proportions at equilibrium. Migration (μ) has a strong effect on the level of polymorphism at equilibrium. The most diverse states are those closest to the instability boundary. Parameters (where not specified): $\lambda = 2$, $\delta = 0.6$, $\sigma = 0.4$.

such that initial conditions determine which of them is reached. We studied the domains of attraction of the equilibria by numerical simulations. For each set of parameters, and for each set of initial conditions $x_1 = x_2 = a$, $y_1 = y_2 = 1-a$ we recorded the state of the system after sufficient time to reach either extinction of one colour type or coexistence (usually $> 10\,000$ steps). The results are shown on Fig. 3. The domain of attraction of stability gets very narrow for high values of the unpalatability parameter. By small stochastic variations in numbers, the system will escape the basin of attraction of coexistence, and shift to a very stable monomorphic state. This means that in reality the tail of the coexistence equilibrium must be truncated at high values of unpalatability. This result is similar for fast migration or weak habitat heterogeneity. Fig. 4 summarizes how the equilibria and their domains of attraction vary with the level of unpalatability λ.

4.5. Asymmetrical cases

Our analysis has concentrated on a case where symmetry allowed an easier analysis of the equations. Symmetry is expected to be more favourable to the maintenance of polymorphism, so we explored the potential effect on our results of asymmetry in some parameters affecting patch quality or signal efficiency. Keeping average parameters constant, we applied a patch-dependent asymmetry in the abundance of models δ (average mortality differing between the two patches), the migration μ (one patch sending more migrants), and a form-dependent asymmetry in unpalatability λ (one form being better defended and learnt faster). We iterated the dynamics of the system until stabilization, and, as in the symmetrical system, we could not find multiple internal stable equilibria. The results show that

the number of parameter combinations that allow stable polymorphism decreases when compared to the symmetrical case (Fig. 5); this was expected, since asymmetry results in one mimetic form being favoured overall. However, the important observation is that the results remained qualitatively similar to the symmetrical case: for a given level of unpalatability, strong-enough habitat heterogeneity allow the maintenance of polymorphism, and mildly unpalatable mimics can maintain polymorphism over a wider range of parameters (details in the legend of Fig. 5). Therefore, we conclude that our results are not specific to symmetrical equations, and are robust to moderate asymmetry in the parameters.

5. Discussion

Positive density-dependence associated with unpalatability in butterflies is essentially a case of Allee effect, as the net *per capita* growth rate of one form increases with its local density (Allee, 1938). The strength of this effect depends on the prey unpalatability that influences learning and memory in predators (Lindström et al., 1997). However, our equations were designed to fit the density-dependence known from warning-colour systems (Kapan, 2001; Lindström et al., 2001; Mallet and Joron, 1999). This requires a pronounced hyperbolic density-dependence, and with a curvilinearity that increases with the level of unpalatability, which is not found in more general models of Allee effects (e.g. Ferdy and Molofsky, 2002). Whilst being in general accordance with general results on the maintenance of diversity with habitat selection or spatially variable fitness (Hedrick, 1986; Karlin and McGregor, 1972; Levin, 1976) and with recent developments in understanding how spatial vs. local processes influence
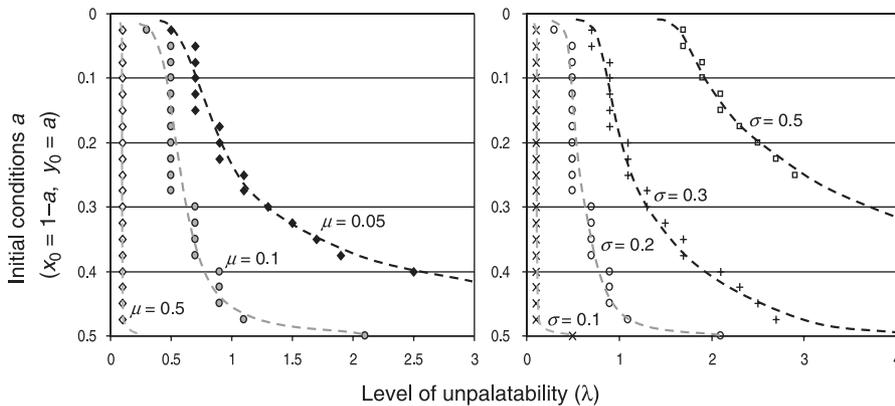

Fig. 3. Domains of attraction. Each point represents the boundary, found by numerical simulations, between the domains of attraction of either exclusion or coexistence. Boundaries are shown as a function of initial conditions a, where $x_0 = a$ and $y_0 = 1-a$ in both patches, for different migration rates μ (left) and for different habitat heterogeneity values σ (right). Below each curve, the system reaches coexistence; above each curve, form B goes extinct. Fixed parameters: left: $\delta = 0.5$, $\sigma = 0.2$; right: $\delta = 0.5$, $\mu = 0.1$. The range of attraction of the coexistence equilibrium gets very thin towards stronger levels of unpalatability λ. The curves were fitted by eye for easier readability only.
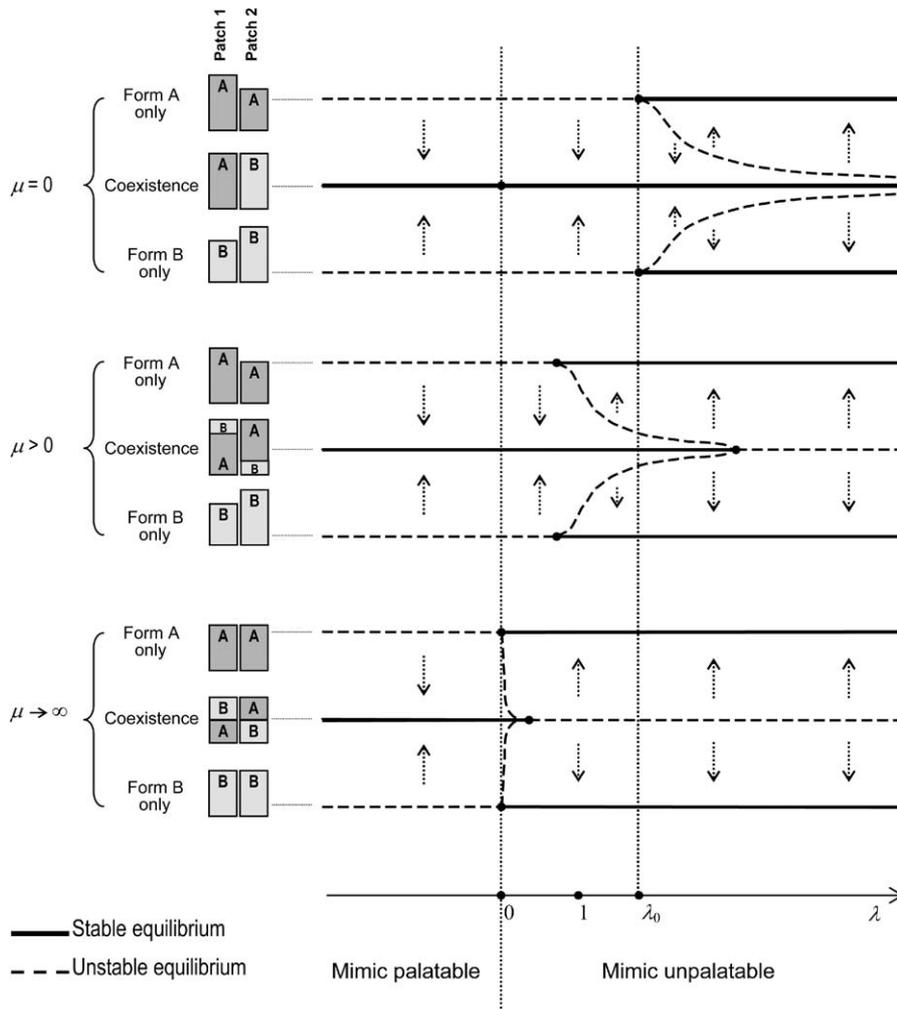
Fig. 4. Distribution of the equilibria as a function of unpalatability (λ) and migration (μ). At null migration, coexistence at the global level is always stable, but not always reachable from a monomorphic state. If migration is not null, there is a threshold value for λ above which no coexistence is stable. For very fast migration, this threshold tends towards 0. For some values of λ, both coexistence and monomorphism are stable; initial conditions will determine which equilibrium is reached. The small bar diagrams to the left give the schematic densities of the mimic's forms A and B in patches 1 and 2 for each equilibrium.

diversity (Amarasekare, 2000; Ferdy and Molofsky, 2002; Nuismer et al., 1999; Switkes and Moody, 2001), our analysis gives important insight into the evolution of diversity in warning colour and mimicry, and, more generally, into the apparently paradoxical maintenance of diversity in traits under positive density-dependence.

5.1. Dynamics of mimicry evolution in an isolated patch

In an isolated patch, two competing mimetic forms cannot coexist, as predicted by the traditional view of Müllerian mimicry. Transient polymorphisms may, however be observed when a form displaces a resident one, a phenomenon called 'mimetic switch' (Turner, 1984). Using coevolutionary equations, Gavrilets and Hastings (1998) also found that transient and/or cyclical Müllerian polymorphisms could be predicted under some circumstances, while stable polymorphisms only

occurred in a distasteful species when a Batesian mimic introduced negative frequency-dependent effects.

In our study, a mimetic switch will only occur if the new form gets stronger protection than the resident one. In other words, the mimic can only switch from the pattern of the rarer model to the commoner model. This condition is, however not sufficient: the mimic's unpalatability must also be low enough, or the difference in abundance between the current model and the alternative one large enough.

This equation may provide an argument against the idea that local mimetic diversity in a place should be constantly eroded due to one large mimicry ring attracting more and more species (Turner, 1995). In particular, independent mimetic changes in (hypothetical) isolated forest fragments have been considered a major mechanism shaping mimetic diversity in butterflies in South America (Turner, 1977; Turner and
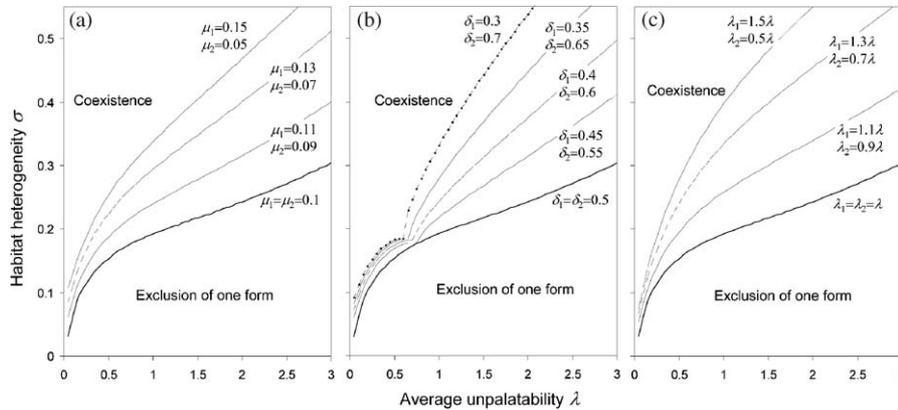
Fig. 5. Coexistence in asymmetrical situations. We iterated the dynamics of the system using patch-dependent values for parameters μ (a) and δ (b), and morph-dependent values for λ (c). The graphs show the stability boundary value of the level of unpalatability λ a function of habitat heterogeneity σ (polymorphism is stable below each curve), for increasing asymmetry in one other parameter while keeping all averages constant ($\delta = 0.5$ and μ). Curves on panel c are for increasing the asymmetry in λ between the two forms, around the average value λ given on the x axis. As expected, the stability boundary shifts towards higher values of σ. When local average mortality δ_j varies between patches (b), heterogeneity in absolute mortality may be reversed for one of the forms ($\delta_1(1+\sigma) < \delta_2(1-\sigma)$)), in which case both forms have higher mortality in the same patch ($\delta_{1A} < \delta_{1B} < \delta_{2B} < \delta_{2A}$). This produces a situation by which the patch where mortality is higher is also where selection for local mimicry is stronger ($\delta_2\sigma > \delta_1\sigma$); this slightly counteracts the adverse effect of asymmetry on coexistence, and results in the shallow hump in the curve on (b). Qualitatively, however, the behaviours of symmetrical and asymmetrical systems remain very similar in all cases.

Mallet, 1996). Our model suggests that these mimetic switches should not occur when the mimic is fairly abundant compared to its models (small δ) or when it is rather strongly protected (large λ). Therefore, it is unlikely that the abundant and very distasteful butterfly *H. erato* diverged into numerous geographical races across South America via independent mimetic switches to match local mimicry rings. This requires the unparsimonious hypothesis that a far more numerous, but now everywhere extinct, model species was present in every putative forest refugium with distinct colour patterns.

At the community level, high local colour-pattern diversity (even abundance of the mimicry rings, local fitness peaks of similar heights) should be slow to erode since changes in pattern should be restricted (σ low, Eq. (6)). Only a relatively skewed colour-pattern distribution (low diversity, one very common pattern) should quickly collapse to a single mimicry ring in the absence of spatial dynamics, since the best protected pattern then becomes very attractive (σ high). Although mimetic switches in nature will also depend on other mechanisms such as the genetic architecture of the traits, this prediction could be explored by simulations, and compared to existing patterns of coexistence in nature.

Finally, the level of unpalatability of the mimic (λ) does influence mimetic changes. In particular, mildly unpalatable species should be rather labile as to their mimetic association, readily adapt to local mimicry, and therefore quickly diversify geographically (see, e.g. Brower, 1996; Mallet et al., 1996; Symula et al., 2001).

5.2. Mimicry in spatially distributed habitats: landscape vs. local scale diversity

When space is considered, strong unpalatability (high λ) tends to stabilize global monomorphism, while strong spatial structure (slow migration, high levels of heterogeneity) and strong selection (high mortality) tend to favour local adaptation to the mimetic environment and the coexistence of mimetic forms in the two-patch system. There is a sudden qualitative switch from protected polymorphism to unstable coexistence as heterogeneity is reduced. As long as landscape-level coexistence is stable, migration between patches mathematically guarantees diversity at the local level; however, such local diversity can be very biased in favour of the locally adapted forms, making local coexistence in some cases biologically irrelevant or undetectable. Consequently, although coexistence and exclusion depend on all factors, some factors have little effect on the phenotypic variance around either equilibrium. For instance, weak unpalatability makes polymorphism more likely at the landscape level, but does not guarantee high levels of local polymorphism (Fig. 2). Only the scale of the spatial structure (μ) and the strength of selection (δ) really affect the level of local diversity at equilibrium. Note that coexistence is possible even without heterogeneity in mimicry, by the sole effect of strong positive density dependence in the aposematic species (Fig. 1b), but this requires rather limited migration between patches and strong selection.

With additional patches, and with asymmetry in some parameters, the conditions for coexistence at the

landscape level may become more restrictive if the overall migration balance is biased towards one form. The maintenance of diversity should therefore depend on the spatial arrangement of the patches, especially on the convexity of the contact zones between alternative habitat types (see simulations and analytical work by Molofsky et al., 2001; Sasaki et al., 2002). In general however, variations in density can maintain balanced clines, or trap them at density troughs (Mallet, 1993; Sasaki et al., 2002), which enhances spatial mosaics. Although it is difficult to draw general predictions as to how asymmetry and complexity might influence coexistence, this suggests that complex heterogeneous environments should make coexistence easier. Finally, Mallet and Barton's (1989) genetic model shows that clines separating alternative mimetic forms, such as those found in *H. melpomene* or *H. erato*, are wider and tend to move more slowly when selection is weak. This means that spatial segregation, and possibly mosaics, should be enhanced with weak selection and frequency-dependence, as in our model. In contrast, the effect of multi-locus genetics and epistasis on spatial coexistence is not straightforward to predict, so we think that the interplay between unpalatability and colour-pattern genetics should be considered an important avenue for future theoretical research on mimicry evolution.

5.3. Local maladaptation

In our model, a locally maladaptive situation occurs when the majority of the focal species in one patch mimics the rarer models.

For coexistence equilibria, this may happen under conditions where the local environment has little differential effect on mimicry (small to null σ, small δ, large λ). However, these conditions represent a narrow zone in the parameter space, and the rest of the coexistence equilibria are stable only when locally adapted. Local adaptation is generally predicted for polymorphic mimics; in case studies, we indeed observe a good correlation of local frequencies between the different forms and their respective models (Joron et al., 1999; Kapan, 2001).

The extinction of one mimetic form is a more common case of maladapative situation, attained with fast migration. Classically, the rise of the locally adapted form will be impeded in one of the populations because strong gene flow from the other population stabilizes one colour pattern in both sites (see e.g. Comins, 1977 for a similar situation with insecticide resistance). Initial conditions thus determine whether the aposematic prey gets trapped in monomorphism, even if local adaptation would ultimately lead to a lower mortality on the whole system.

The recent coevolutionary equations analysed by Gomulkiewicz et al. (2000) and Nuismer et al. (1999)

led to similar results (although the absence of intraspecific effects makes their application to warning colour only partial). Polymorphisms were maintained easily under limited migration and strong local selection, allowing for local adaptation, while fast migration and weak selection resulted in one patch type dictating the global dynamics, as in our and previous model. Spatial coevolutionary simulations of Müllerian mimicry would be an interesting extension of our equations.

5.4. Unpalatability and the position of the Batesian/Müllerian boundary

Polymorphism appears more likely in mildly unpalatable species than in strongly unpalatable species. This result is similar, but for different reasons, to that of other studies that suggested that mildly unpalatable species may act as parasites of their models, leading to Batesian-like adaptive polymorphism. Huheey (1976, 1988) suggested that the Batesian/Müllerian mimicry boundary was not necessarily situated at the point of zero—or neutral—unpalatability of the mimic, but at the point where both mimicking species have exactly equal unpalatability, making Müllerian mimicry a purely theoretical case. Speed (1993) suggested that a transition zone between true Batesian mimicry and true Müllerian mimicry, defined as "quasi-Batesian mimicry", was characterized by negative frequency-dependence (Batesian dynamics) in mildly unpalatable mimics.

The realism and evolutionary implications of these distinctions are debated elsewhere (Joron and Mallet, 1998; Lindström et al., 2001; Mallet, 1999; Mallet and Joron, 1999; Speed, 2001; Speed et al., 2000; Speed and Turner, 1999). However, taking space into account may shortcut the controversy. As in many cases where discrepancies between empirical data and panmictic-population theory could be clarified by considering spatial dynamics (e.g. Cheptou and Mathias, 2001), our model predicts that, by the sole effect of spatial dynamics, mildly distasteful species may maintain polymorphism where nastier species may not.

Here, if spatial structure is ignored as in previous single-population models, the monomorphism/polymorphism boundary is set at zero palatability (barred area on Fig. 6): this is the classical view of mimicry. However, such a homogeneous environment is purely theoretical. As soon as some spatial variation is added to the model, the boundary between monomorphism and polymorphism starts extending into the "unpalatability" domain of the spectrum (Fig. 6): the stronger the spatial structure (higher habitat heterogeneity for a given level of dispersal), the easier the coexistence.

Through self-reinforcement, strongly distasteful species (high λ) become independent of local mimicry on a broader set of environmental parameters (σ and δ) than
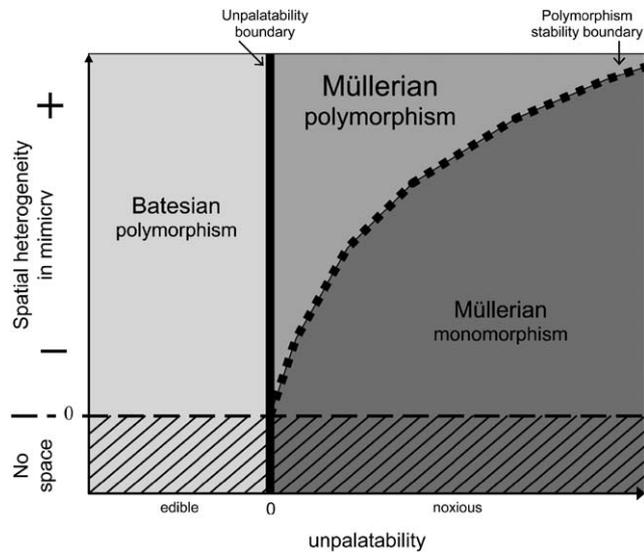
Fig. 6. Polymorphism and the palatability spectrum. If space is ignored (barred area) the polymorphism boundary coincides with the palatability boundary. If space is considered, a polymorphic area (medium grey) extends into the unpalatable side of the spectrum, despite local positive density-dependence.

milder species. Therefore, mild species are more likely than stronger species to adapt locally (see single patch), and very low levels of spatial heterogeneity are sufficient to maintain a migration-selection balance at the landscape level. Moreover, in a strongly distasteful species, polymorphism is stable in a narrower zone, and any small variation in habitat heterogeneity (σ) can bring the global system into the range of attraction of monomorphism (Fig. 3). Therefore, polymorphism in a strongly unpalatable species is predicted to remain only if the pattern of habitat heterogeneity is especially stable in time (see Section 5 below), further restricting the evolution of stable polymorphism in these species.

In our view, the interplay between unpalatability and the spatial structure of selection provides an alternative and parsimonious explanation for the transition zone between polymorphic Batesian mimics and monomorphic Müllerian mimics, simply because mildly distasteful species can evolve polymorphism on a broader set of ecological situations. Polymorphism can evolve in the face of local positive density-dependence, that is, although the mimic is not locally selected for polymorphism. Therefore, that some polymorphic Müllerian species such as the two-spot labybird *Adalia bipunctata* (Marples et al., 1989) or the butterfly *Laparus doris* (Turner, 1971) appear to be mildly distasteful do not support of the reality of quasi-Batesian mimicry (Speed, 1993): instead, even when spatial heterogeneity is relatively low, mild species are particularly likely to evolve polymorphisms, without quasi-Batesian effects.

The implications of this result are important for our understanding of the mechanisms underlying the evolu-

tion of diversity in mimicry systems: indeed, the evolution of polymorphism in an unpalatable mimic may not depend on deleterious effects on the signal efficiency via hypothetical quasi-Batesian effects, so long as local self-reinforcement (selection for monomorphism) is stronger than the homogenizing effect of migration (Fig. 3).

5.5. Polymorphic mimetic butterflies

Many aposematic species display some level of polymorphism, often restricted to narrow hybrid zones, and stabilized by frequency-dependence on either side of steep clines (Mallet, 1993; Mallet et al., 1990). However, some mimetic distasteful butterflies are polymorphic over wide areas, such as the butterflies *Danaus chrysippus* in Africa and *H. numata* and *L. doris* in South America. The migrant *D. chrysippus* is polymorphic in a zone that may be a broad contact zone between vast areas of colour-pattern purity (Smith et al., 1997). In contrast, *H. numata* maintains 2–10 sympatric forms nearly in its whole distribution range (Brown, 1976), each of which participates in a different mimetic association with ithomiine and danaine butterflies. Brown and Benson (1974) hypothesized that polymorphism is an adaptive response of *H. numata* to the spatio-temporal unpredictability of its mimetic environment.

The distastefulness of *H. numata* is unknown, but there is little reason to doubt that it is rather strongly unpalatable (moderate-large λ), as are closely related *H. ismenius*, *H. ethilla* and *H. hecale* (Brower et al., 1963; Srygley and Chai, 1990 a,b; see Joron et al., 1999 for discussion). When handled, males and females release chemical smells by wide-opening claspers or extruding yellow scent glands, as is typical of strongly distasteful insects. Our model predicts that polymorphism in *H. numata* could evolve if the environment is sharply heterogeneous in space and rather stable in time. In *H. numata*, a measure of the heterogeneity of the mimetic environment is given by the variation in local colour-pattern frequencies of the co-mimetic species *Melinaea* spp.: the mimetic environment was found to be strongly heterogeneous in space (large σ), with sites less than 10 km apart being dominated by radically different mimicry rings, with indications of local selection for mimicry (Joron et al., 1999). This spatial pattern was found to be stable in time over the 3-year period of this study (12–18 generations), and some evidence suggest that it is stable even on a 15-year period or more (Mallet, Lamas, Joron, unpubl. data). Since the colour-pattern in this species is inherited as a monogenic character (Brown and Benson, 1974; Joron, 2000), Joron et al. (1999) concluded that the polymorphism in *H. numata* is the mere result of multiple clines at a single-locus maintained by a migration-selection balance.

These results are fully consistent with the predictions of our model.

Besides, the high and spatially homogeneous allozyme diversity suggest *H. numata* is fairly dispersive (Joron et al., 1999), as are the related species *H. erato* and *H. melpomene* (Mallet, 1986a; Mallet et al., 1990). Nevertheless, the frequencies of the different forms of *H. numata* were found to be spatially very well correlated to the local frequencies of their respective co-mimics *Melinaea* spp. even when nearby sites were selected for distinct colour patterns, showing local adaptation of *H. numata* to its mimetic environment. Under fast migration, our model again predicts such a local adaptation. Similarly, in other polymorphic species like *H. cydno* (Kapan, 2001; Linares, 1994) or *L. doris* (Mallet, 1999), the frequencies of the different forms are correlated to those of the respective models, although the correlation is on a wider geographic scale and the changes more gradual than in *H. numata*. Finally, sex-specific micro-habitat use such as that observed in polymorphic *H. numata* and *H. cydno*, may facilitate local adaptation (Joron, 2005; Merchán et al., 2005), which in turn enhances the importance of spatial variation in the maintenance of polymorphism in Müllerian mimics.

5.6. Conclusions: Positive density dependence and diversity

Traits under positive density-dependence are not predicted to evolve stable polymorphisms in single populations, in the absence of other balancing factors, such as unequal competitive abilities (Ferdy and Molofsky, 2002). However, although local density-dependence destabilizes coexistence, spatial processes can in many circumstances preserve coexistence at the landscape scale by stabilizing the geographical segregation of forms (Amarasekare, 2000; Molofsky et al., 2001). The scale of this segregation compared to the dispersal abilities of the species involved will determine the level of local polymorphism that can be attained. In some instances, spatial segregation can be very fine-grained, resulting in a mosaic of populations dominated by alternative forms, but with considerable mixing and, therefore, local polymorphism (Joron et al., 1999). Positive density-dependence has this interesting property that, although a resident form may be protected from replacement by other phenotypes, all phenotypes are a priori equally robust to replacement once established. This means that if temporary relaxing in the density-dependent mechanisms (here: fluctuations in predator populations or in habitat heterogeneity) result in phenotypic shifts in some populations via local drift or migration, novel or alien phenotypes can repeatedly pop-up as pockets in the landscape, which resist further replacements, and can potentially expand (Mallet and Barton, 1989; Molofsky et al., 2001; Sasaki et al., 2002).

Thus, despite favouring local monomorphism, positive density-dependence can strongly contribute to a higher diversity at the landscape level.

Acknowledgements

Appendix A. Analysis for a single patch

A.1. Condition for a rare form to displace a locally maladapted form

Let $\hat{y}_0^{(B)}$ be the equilibrium density reached by form B alone in a single patch with $\delta_B > \delta_A$, i.e. defined by the second line of Eq. (4) in text with $x_0 = 0$:

$$\hat{y}_0^{(B)} = 1 - \frac{\delta_B}{1 + \lambda \hat{y}_0^{(B)}}. \tag{A.1}$$

The condition for form A invading the patch is $\delta_B > \delta_A(1 + \lambda \hat{y}_0^{(B)})$. Because $\hat{y}_0^{(B)}$ increases as λ increases and as mortality decreases, there may exist a threshold value for λ, λ_0, above which A cannot invade

$$\lambda_0 = \frac{\delta_{B1} - \delta_{A1}}{\delta_{A1}(1 - \delta_{A1})}.$$

Appendix B. Two patches, exclusion of one form

B.1. Invasibility condition

If only mimics of form A are present, and provided that mortality is sufficiently low to allow the populations to be maintained in both patches ($\delta < 1$), A will reach the equilibrium $(\hat{x}_1, \hat{x}_2)$, defined by the first and third lines of Eq. (3) in text, with $y_1 = 0$ and $y_2 = 0$. Obviously, $\hat{x}_1$ is higher than $\hat{x}_2$ because of a lower mortality for form A in patch 1. When y_1 and y_2 are very small, their differential equations become

$$\frac{d}{d\tau}\begin{pmatrix} y_1 \\ y_2 \end{pmatrix} = \begin{pmatrix} -\delta_L + 1 - \hat{x}_1 - \mu & \mu \\ \mu & -\delta_S + 1 - \hat{x}_2 - \mu \end{pmatrix}\begin{pmatrix} y_1 \\ y_2 \end{pmatrix}. \tag{B.1}$$

Type B mimics can then establish in the system if and only if the dominant eigenvalue of the transition matrix

in Eq. (B.1) is positive, that is, only if Eq. (7) in text holds.

B.2. Exclusion of one form for very fast migration

When the migration rate μ is very large, the difference between x_1 and x_2 would quickly become very small (of the magnitude of $1/\mu$). Then, by contracting the equations for their average, we can derive that both x_1 and x_2 would approximately converge to the value $\hat{x}_\infty^{(A)}$ defined by

$$1 - \hat{x}_\infty^{(A)} = \frac{\delta_\infty}{1 + \lambda \hat{x}_\infty^{(A)}}, \tag{B.2}$$

in which δ_∞ is the average of δ_S and δ_L [i.e. $\delta_\infty = (\delta_S + \delta_L)/2$]. The equilibrium $\{(\hat{x}_1, 0), (\hat{x}_2, 0)\}$ reached by form A alone ($y = 0$) can be written $\hat{x}_1 = \hat{x}_\infty^{(A)} + \varepsilon$ and $\hat{x}_2 = \hat{x}_\infty^{(A)} - \kappa$, where ε and κ are of the order of $1/\mu$. The invasibility condition given by Appendix B.1 is therefore

$$\left(-\delta_L + 1 - \hat{x}_\infty^{(A)} - \varepsilon\right)\left(-\delta_S + 1 - \hat{x}_\infty^{(A)} + \kappa\right)$$
$$- \mu\left(-\delta_S - \delta_L + 2 - 2\hat{x}_\infty^{(A)} - \varepsilon + \kappa\right) < 0 \tag{B.3}$$

When μ tends to infinity, the sign of the left-hand side of inequality (B.3) is that of the leading term in μ. Therefore, the invasibility condition becomes

$$-\delta_S - \delta_L + 2 - 2\hat{x}_\infty^{(A)} - \varepsilon + \kappa > 0. \tag{B.4}$$

Using the definitions of δ_∞ and $\hat{x}_\infty^{(A)}$, we can rewrite inequality (B.4) as $-2\lambda\delta_\infty\hat{x}_\infty^{(A)}/(1 + \lambda\hat{x}_\infty^{(A)}) + \varepsilon - \kappa > 0$, which cannot hold if λ is positive, because we assume ε and κ are both small. Hence a new form can never invade.

Appendix C. Two patches, coexistence

C.1. Existence of several coexistence equilibria

With null habitat heterogeneity ($\sigma = 0$), and when coexistence is stable, two alternative stable coexistence equilibria exist where the two patches are fixed or dominated by alternative forms (see text). For two stable equilibria to be possible, λ has to be large enough ($\lambda > \lambda_1$) for local density-dependence to offset migration and habitat difference when $\sigma \neq 0$, and small enough ($\lambda < \lambda_2$) for global coexistence to be stable. When $\sigma = 0$, the unstable coexistence equilibrium **E** is fully symmetrical, with $\hat{x}_1 = \hat{x}_2 = \hat{y}_1 = \hat{y}_2$ (<0.5). Since $\sigma = 0$, the two alternative coexistence equilibria are stable for the same values of parameters; hence we are looking for the conditions where the unstable equilibrium **E** splits

into 3 equilibria. With $\sigma = 0$, λ_1 and λ are found when

$$\hat{y} = \hat{x}$$
$$\left.\frac{\mathrm{d}f(\hat{x})}{\mathrm{d}\hat{x}}\right|_{\lambda = \lambda_1, \lambda_2} = 1, \quad \text{where}$$
$$f(\hat{x}) = \hat{y}$$
$$= \left(\frac{\hat{x}}{\hat{x} - \mu}\right)\left(\frac{-\delta}{1 + \lambda\hat{x}} + 1 - \hat{x} - \mu\right). \tag{C.1}$$

Analytical resolution of Eq. (C.1) shows that λ_1 and λ_2 exists only if $\delta \geq 8\mu$. Therefore, since $0 < \delta < 1$ (for the two patches to be viable), there can be several coexistence equilibria only if $\mu < 0.125$, i.e. when μ is sufficiently small. When, $\mu > \delta/8$, only one coexistence equilibrium is possible, the $\delta > 8\mu$, the range where several coexistence equilibria exist is bounded by two values λ_1 and λ_2. When $\sigma = 0$ and $\mu = 0$, the two patches are isolated, so $\lambda_1 = \lambda_0 = 0$ and $\lambda_2 \to +\infty$, whence three coexistence equilibria (two stable and one unstable) exist for all positive values of λ. Isoclines on Fig. 7 show how one equilibrium splits into three equilibria as migration becomes very small.

C.2. Stability condition for symmetrical coexistence

Around the symmetrical equilibria, the Jacobi matrix of the system, $\mathbf{J}_{sym}$, can be written as:

$$\mathbf{J}_{sym} = \begin{bmatrix} P & -\hat{x} & \mu & 0 \\ -\hat{y} & Q & 0 & \mu \\ \mu & 0 & Q & -\hat{y} \\ 0 & \mu & -\hat{x} & P \end{bmatrix}, \quad \text{where}$$
$$\begin{cases} P = \dfrac{-\delta_S}{(1 + \lambda\hat{x})^2} + 1 - 2\hat{x} - \hat{y} - \mu, \\[2mm] Q = \dfrac{-\delta_L}{(1 + \lambda\hat{y})^2} + 1 - 2\hat{y} - \hat{x} - \mu. \end{cases} \tag{C.2}$$

Setting the transform $\xi_1 = x_1 + y_2$, $\xi_2 = y_1 + x_2$, $\eta_1 = x_1 - y_2$, $\eta_2 = y_1 - x_2$, the system becomes:

$$\frac{\mathrm{d}}{\mathrm{d}\tau}\begin{pmatrix} \xi_1 \\ \xi_2 \\ \eta_1 \\ \eta_2 \end{pmatrix} = \begin{pmatrix} P & -\hat{x} + \mu & 0 & 0 \\ -\hat{y} + \mu & Q & 0 & 0 \\ 0 & 0 & P & -\hat{x} - \mu \\ 0 & 0 & -\hat{y} - \mu & Q \end{pmatrix}$$
$$\times \begin{pmatrix} \xi_1 \\ \xi_2 \\ \eta_1 \\ \eta_2 \end{pmatrix}. \tag{C.3}$$

The stability analysis of the matrix above can be decomposed of the analysis of two 2×2 submatrices.
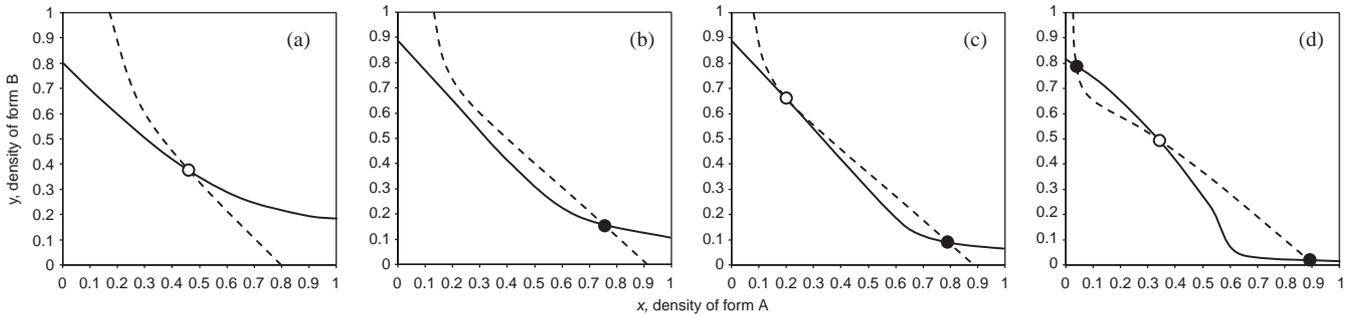
Fig. 7. Phase diagrams of the two-patch model. The dashed line is the isoclines for form A (density of A at equilibrium in patch 1); the solid line is the isocline for form B (in patch 1). As migration decreases (diagrams *a* to *d*, $\mu = 0.1, 0.05, 0.033, 0.01$), the unstable coexistence equilibrium (a, open circle) becomes stable (b, solid circle), then two additional internal equilibria appear (c and d), one stable, one unstable. Other parameters: $\delta = 0.6$, $\sigma = 0.45$, $\lambda = 5$.

Hence, the system is stable if and only if the following three inequalities hold:

$$P + Q < 0,$$
$$PQ - (\hat{x} - \mu)(\hat{y} - \mu) > 0,$$
$$PQ - (\hat{x} + \mu)(\hat{y} + \mu) > 0. \tag{C.4}$$

The second inequality is satisfied if the third inequality holds. Besides, all the cases we studied for the shape of the stability boundary satisfied $P + Q < 0$, though we could not prove it in general. Hence the stability condition is the third inequality in Eq. (C.4).

C.3. Unstable coexistence for very fast migration

Let us consider the same single big patch as in Appendix B, where the mortality parameter is $\delta_{\infty} = (\delta_S + \delta_L)/2$ for both forms (in other words, $\sigma = 0$). Because of this symmetry, the only internal equilibrium is $\hat{x}_{\infty}(= \hat{x}_1 = \hat{y}_1)$, defined by

$$\frac{-\delta}{1 + \lambda \hat{x}_{\infty}} + 1 - 2\hat{x}_{\infty} = 0 \tag{C.5}$$

This equilibrium is unstable (Appendix A).

In a two-patch system, let us now consider the case where $\mu \to +\infty$. The internal equilibrium can be written $(\hat{x}, \hat{y}) = (\hat{x}_{\infty} + \varepsilon, \hat{x}_{\infty} - \kappa)$, where ε and κ are small entities of the order of $(1/\mu)$. The stability condition of this equilibrium can be written

$$-\mu G + o(\mu) > 0, \quad \text{where } G \text{ is a function of } \hat{x}_{\infty}, \delta_S,$$
$$\delta_L, \lambda, \varepsilon \text{ and } \kappa. \tag{C.6}$$

If μ is very large, Eq. (C.6) is equivalent to $G < 0$. Using Eq. (C.5), $G < 0$ becomes

$$(1 - 2\hat{x}_{\infty}) \frac{\lambda \hat{x}_{\infty}}{1 + \lambda \hat{x}_{\infty}} < 0. \tag{C.7}$$

Since $\hat{x}_{\infty} < 0.5$, Eq. (C.7) is never verified if $\lambda > 0$, and always verified if $-1/\hat{x}_{\infty} < \lambda < 0$. We conclude that for $\mu \to +\infty$, the internal equilibrium is unstable for all positive values of λ, and always stable for negative values of λ.

References

Allee, W.C., 1938. The Social Life of Animals. William Heinemann, London.

Amarasekare, P., 2000. The geometry of coexistence. Biol. J. Linn. Soc. 71, 1–31.

Ayala, F.J., Campbell, C.A., 1974. Frequency-dependent selection. Ann. Rev. Ecol. Syst. 5, 115–138.

Bates, H.W., 1862. Contributions to an insect fauna of the Amazon valley. Lepidoptera: Heliconidae. Trans. Linn. Soc. London 23, 495–566.

Beccaloni, G.W., 1997. Ecology, natural history and behaviour of ithomiine butterflies and their mimics in Ecuador (Lepidoptera: Nymphalidae: Ithomiinae). Trop. Lepidoptera 8, 103–124.

Benson, W.W., 1972. Natural selection for Müllerian mimicry in *Heliconius erato* in Costa Rica. Science 176, 936–939.

Bever, J.D., 1999. Dynamics within mutualism and the maintenance of diversity: inference from a model of interguild frequency dependence. Ecol. Lett. 2, 52–62.

Brower, A.V.Z., 1996. Parallel race formation and the evolution of mimicry in *Heliconius* butterflies: a phylogenetic hypothesis from mitochondrial DNA sequences. Evolution 50, 195–221.

Brower, L.P., Brower, J.V.Z., Collins, C.T., 1963. Experimental studies of mimicry, 7: relative palatability and Müllerian mimicry among Neotropical butterflies of the subfamily Heliconiinae. Zoologica (New York) 48, 65–84.

Brown, K.S., 1976. An illustrated key to the silvaniform *Heliconius* (Lepidoptera: Nymphalidae) with descriptions of new subspecies. Trans. Am. Entomol. Soc. 102, 373–484.

Brown, K.S., Benson, W.W., 1974. Adaptive polymorphism associated with multiple Müllerian mimicry in *Heliconius numata*. Biotropica 6, 205–228.

Chai, P., 1986. Field observations and feeding experiments on the responses of rufous-tailed jacamars (*Galbula ruficauda*) to free-flying butterflies in a tropical rainforest. Biol. J. Linn. Soc. 29, 161–189.

Cheptou, P.O., Mathias, A., 2001. Can varying inbreeding depression select for intermediary selfing rates? Am. Nat. 157, 361–373.

Chesson, P., 2000. Mechanisms of maintenance of species diversity. Annu. Rev. Ecol. Syst. 31, 343–366.

Comins, H.N., 1977. The development of insecticide resistance in the presence of migration. J. Theor. Biol. 64, 177–197.

Courchamps, F., Clutton-Brock, T., Grenfell, B., 1999. Inverse density denpendence and the Allee effect. Trends Ecol. Evol. 14, 405–410.

Endler, J.A., 1988. Frequency-dependent predation, crypsis, and aposematic coloration. Philos. Trans. R. Soc. London Ser. B 319, 505–522.

Ferdy, J.-B., Molofsky, J., 2002. Allee effect, spatial structure and species coexistence. J. Theor. Biol. 217, 413–424.

Flanagan, N., Tobler, A., Davison, A., Pybus, O.G., Kapan, D.D., Planas, S., Linares, M., Heckel, D., McMillan, W.O., 2004. The historical demography of Müllerian mimicry in the Neotropical *Heliconius* butterflies. Proc. Natl Acad. Sci USA 101, 9704–9709.

Gavrilets, S., Hastings, A., 1998. Coevolutionary chase in two-species systems with applications to mimicry. J. Theor. Biol. 191, 415–427.

Gigord, L.D.B., Macnair, M.R., Smithson, A., 2001. Negative frequency-dependent selection maintains a dramatic flower color polymorphism in the rewardless orchid *Dactylorhiza sambucina* (L.) Soò. Proc. Natl Acad. Sci USA 98, 6253–6255.

Gomulkiewicz, R., Thompson, J.N., Holt, R.D., Nuismer, S.L., Hochberg, M.E., 2000. Hot spots, cold spots, and the geographic mosaic theory of coevolution. Am. Nat. 156, 156–174.

Gordon, I.J., Smith, D.A.S., 1998. Body size and colour-pattern genetics in the polymorphic mimetic butterfly *Hypolimnas misippus* (L.). Heredity 80, 62–69.

Haldane, J.B.S., Jayakar, S.D., 1963. Polymorphism due to selection depending on the composition of a population. J. Hered. 58, 318–323.

Hedrick, P.W., 1986. Genetic polymorphism in heterogeneous environments: a decade later. Annu. Rev. Ecol. Syst. 17, 535–566.

Huheey, J.E., 1976. Studies of warning coloration and mimicry, VII: evolutionary consequences of a Batesian–Müllerian spectrum: a model for Müllerian mimicry. Evolution 30, 86–93.

Huheey, J.E., 1988. Mathematical models of mimicry. Am. Nat. 131, S22–S41.

Joron, M., 2000. Warning colour and Müllerian mimicry: the diversification puzzle. Ph.D. Dissertation. Département Biologie, Evolution, Environnement, Université de Montpellier, France. 225 pp.

Joron, M., 2005. Polymorphic mimicry microhabitat use and sex-specific behaviour. J. Evol. Biol. 18, 547–556.

Joron, M., Mallet, J., 1998. Diversity in mimicry: paradox or paradigm? Trends in Ecol. Evol. 13, 461–466.

Joron, M., Wynne, I.R., Lamas, G., Mallet, J., 1999. Variable selection and the coexistence of multiple mimetic forms of the butterfly *Heliconius numata*. Evol. Ecol. 13, 721–754.

Kapan, D.D., 2001. Three-butterfly system provides a field test of Müllerian mimicry. Nature 409, 338–340.

Karlin, S., McGregor, J., 1972. Polymorphisms for genetic and ecological systems with weak coupling. Theor. Popul. Biol. 3, 186–209.

Levin, S.A., 1976. Population dynamic models in heterogeneous environments. Annu Rev. Ecol. Syst. 7, 287–310.

Linares, M., 1994. Origin of Neotropical mimetic biodiversity from a three-way hybrid zone of *Heliconius cydno* butterflies. In: Proceedings of the International Symposium on Biodiversity and Systematics in Tropical Ecosystems, Zoologisches Forschungsinstitut und Museum Alexander Koenig, Bonn. pp. 93–108.

Lindström, L., Alatalo, R.V., Mappes, J., 1997. Imperfect Batesian mimicry—the effects of the frequency and the distastefulness of the model. Proc. R. Soc. London Ser. B: Biol. Sci. 264, 149–153.

Lindström, L., Alatalo, R.V., Lyytinen, A., Mappes, J., 2001. Strong antiapostatic selection against novel rare aposematic prey. Proc. Natl Acad. Sci. USA 98, 9181–9184.

Mallet, J., 1986a. Dispersal and gene flow in a butterfly with home range behaviour: *Heliconius erato* (Lepidoptera: Nymphalidae). Oecologia 68, 210–217.

Mallet, J., 1986b. Hybrid zones of *Heliconius* butterflies in Panama and the stability and movement of warning colour clines. Heredity 56, 191–202.

Mallet, J., 1993. Speciation, raciation, and color pattern evolution in *Heliconius* butterflies: Evidence from hybrid zones. In: Harrisson, R.G. (Ed.), Hybrid Zones and the Evolutionary Process. Oxford University Press, New York, pp. 226–260.

Mallet, J., 1999. Causes and consequences of a lack of coevolution in Müllerian mimicry. Evol. Ecol. 13, 777–806.

Mallet, J., Barton, N., 1989. Inference from clines stabilized by frequency-dependent selection. Genetics 122, 967–976.

Mallet, J., Joron, M., 1999. Evolution of diversity in warning color and mimicry: polymorphisms, shifting balance and speciation. Annu. Rev. Ecol. Syst. 30, 201–233.

Mallet, J., Barton, N.H., Lamas, G., Santisteban, C.J., Muedas, M.M., Eeley, H., 1990. Estimates of selection and gene flow from measures of cline width and linkage disequilibrium in *Heliconius* hybrid zones. Genetics 124, 921–936.

Mallet, J., Jiggins, C.D., McMillan, W.O., 1996. Evolution: mimicry meets the mitochondrion. Curr. Biol. 6, 937–940.

Marples, N.M., Brakefield, P.M., Cowie, R.J., 1989. Differences between the 7-spot and 2-spot ladybird beetles (Coccinellidae) in their toxic effects on a bird predator. Ecol. Entomol. 14, 79–84.

Merchán, A., Jiggins, C.D., Linares, M., 2005. A narrow *Heliconius cydno* (Nymphalidae; Heliconiini) hybrid zone with differences in morph sex ratios. Biotropica 37, 118–127.

Molofsky, J., Bever, J.D., Antonovics, J., 2001. Coexistence under positive frequency dependence. Proc. R. Soc. London Ser. B: Biol. Sci. 268, 273–277.

Müller, F., 1879. *Ituna* and *Thyridia*: a remarkable case of mimicry in butterflies. Trans. Entomol. Soc. London 1879, xx–xxix.

Nowak, M.A., Krakauer, D.C., 1999. The evolution of language. Proc. Natl Acad. Sci USA 96, 8028–8033.

Nuismer, S.L., Thompson, J.N., Gomulkiewicz, R., 1999. Gene flow and geographically structured coevolution. Proc. R. Soc. London Ser. B 266, 605–609.

Owen, R.E., Owen, A.R.G., 1984. Mathematical paradigms for mimicry: recurrent sampling. J. Theor. Biol. 109, 217–247.

Plowright, R.C., Owen, R.E., 1980. The evolutionary significance of bumble bee colour patterns: a mimetic interpretation. Evolution 34, 622–637.

Sasaki, A., Kawagushi, I., Yoshimori, A., 2002. Spatial mosaic and interfacial dynamics in Müllerian mimicry system. Theor. Popul. Biol. 61, 49–71.

Smith, D.A.S., Owen, D.F., Gordon, I.J., Lowis, N.K., 1997. The butterfly *Danaus chrysippus* (L.) in East Africa: polymorphism and morph-ratio clines within a complex, extensive, and dynamic hybrid zone. Zool. J. Linn. Soc. 120, 51–78.

Smithson, A., Macnair, M.R., 1997. Density-dependent and frequency-dependent selection by bumblebees *Bombus terrestris* (L) (Hymenoptera: Apidae). Biol. J. Linn. Soc. 60, 401–417.

Speed, M.P., 1993. Müllerian mimicry and the psychology of predation. Anim. Behav. 45, 571–580.

Speed, M.P., 2001. Batesian, quasi-Batesian or Müllerian mimicry? Theory and data in mimicry research. Evol. Ecol. 13, 755–776.

Speed, M.P., Turner, J.R.G., 1999. Learning and memory in mimicry, II: do we understand the mimicry spectrum? Biol. J. Linn. Soc. 67, 281–312.

Speed, M.P., Alderson, N.J., Hardman, C., Ruxton, G.D., 2000. Testing Müllerian mimicry: and experiment with wild birds. Proc. R. Soc. London Ser. B 267, 725–731.

Srygley, R.B., Chai, P., 1990a. Flight morphology of Neotropical butterflies: palatability and distribution of mass to the thorax and abdomen. Oecologia 84, 491–499.

Srygley, R.B., Chai, P., 1990b. Predation and the elevation of thoracic temperature in brightly colored Neotropical butterflies. Am. Nat. 135, 766–787.

Switkes, J.M., Moody, M.E., 2001. Coevolutionary interactions between a haploid species and a diploid species. J. Math. Biol. 42, 175–194.

Symula, R., Schulte, R., Summers, K., 2001. Molecular phylogenetic evidence for a mimetic radiation in Peruvian poison frogs supports a Müllerian mimicry hypothesis. Proc. R. Soc. London Ser. B 268, 2415–2421.

Tilman, D., 1990. Constraints and tradeoffs—toward a predictive theory of competition and succession. Oikos 58, 3–15.

Turner, J.R.G., 1971. Studies of Müllerian mimicry and its evolution in burnet moths and heliconid butterflies. In: Creed, E.R. (Ed.), Ecological Genetics and Evolution. Blackwell, Oxford, pp. 224–260.

Turner, J.R.G., 1977. Butterfly mimicry: the genetical evolution of an adaptation. Evol. Biol. 10, 163–206.

Turner, J.R.G., 1984. Mimicry: the palatability spectrum and its consequences. In: Vane-Wright, R.I., Ackery, P.R. (Eds.), The Biology of Butterflies, vol. 11. Academic Press, London, pp. 141–161.

Turner, J.R.G., 1995. Mimicry as a model for coevolution. In: Arai, R., Kato, M., Doi, Y. (Eds.), Biodiversity and Evolution. The National Science Museum Foundation, Tokyo, pp. 131–150.

Turner, J.R.G., Mallet, J., 1996. Did forest islands drive the biodiversity of warningly coloured butterflies? Biotic drift and the shifting balance. Philos. Trans. R. Soc. London Ser. B 351, 835–845.

Turner, J.R.G., Speed, M.P., 1996. Learning and memory in mimicry, I: simulations of laboratory experiments. Philos. Trans. R. Soc. London Ser. B 351, 1157–1170.

Turner, J.R.G., Kearney, E.P., Exton, L.S., 1984. Mimicry and the Monte Carlo predator: the palatability spectrum and the origins of mimicry. Biol. J. Linn. Soc. 23, 247–268.

West, D.A., 1994. Unimodal Batesian polymorphism in the Neotropical swallowtail butterfly *Eurytides lysithous* (Hbn.). Biol. J. Linn. Soc. 52, 197–224.